Acta Crystallographica Section F
Structural Biology and Crystallization Communications
ISSN 1744-3091

Crystallization and preliminary X-ray crystallographic analysis of ligand-free and arginine-bound forms of *Thermotoga maritima* arginine-binding protein

Alessia Ruggiero,[a]* Jonathan D. Dattelbaum,[b] Anna Pennacchio,[c] Luisa Iozzino,[c] Maria Staiano,[c] Matthew S. Luchansky,[b] Bryan S. Der,[b] Rita Berisio,[a] Sabato D'Auria[c] and Luigi Vitagliano[a]*

[a]Institute of Biostructures and Bioimaging, CNR, Via Mezzocannone 16, I-80134 Naples, Italy, [b]Department of Chemistry, University of Richmond, Richmond, VA 23173, USA, and [c]Laboratory for Molecular Sensing, IBP–CNR, Naples, Italy

Correspondence e-mail: alessia.ruggiero@unina.it, luigi.vitagliano@unina.it

Received 22 July 2011
Accepted 13 September 2011

The arginine-binding protein from *Thermotoga maritima* (TmArgBP) is an arginine-binding component of the ATP-binding cassette (ABC) transport system in this hyperthermophilic bacterium. This protein is endowed with an extraordinary stability towards thermal and chemical denaturation. Its structural characterization may provide useful insights for the clarification of structure–stability relationships and for the design of new biosensors. Crystallization trials were set up for both arginine-bound and ligand-free forms of TmArgBP and crystals suitable for crystallographic investigations were obtained for both forms. Ordered crystals of the arginine adduct of TmArgBP could only be obtained by using the detergent LDAO as an additive to the crystallization medium. These crystals were hexagonal, with unit-cell parameters a = 78.2, c = 434.7 Å, and diffracted to 2.7 Å resolution. The crystals of the ligand-free form were orthorhombic, with unit-cell parameters a = 51.8, b = 91.9, c = 117.9 Å, and diffracted to 2.25 Å resolution.

1. Introduction

In many living organisms, the passage of small ligands through the cell membrane is mediated by complex macromolecular assemblies named ATP-binding cassettes (ABCs; Higgins, 1992; Oldham *et al.*, 2008). ABC transport systems constitute a large superfamily of proteins which couple the hydrolysis of ATP to the passage of metabolites through the cell membrane (Ethayathulla *et al.*, 2008). The expressed ABC transporters consist of two transmembrane domains and two ATP-binding domains for the transportation of a specific ligand across the membrane. In Gram-negative bacteria, each transporter relies on a soluble periplasmic binding protein (PBP) that is capable of interacting with a specific ligand essential for metabolic and nutrient gathering (Davidson *et al.*, 2008; Nanavati *et al.*, 2005). The PBPs associated with ABC transport systems are of remarkable interest for the development of protein-based biosensors (de Lorimier *et al.*, 2002; Marvin *et al.*, 1997). Indeed, owing to the variety of their binding specificities, they are currently utilized as designated platforms for fluorescent protein biosensors for many naturally occurring ligands (sugars, anions, amino acids *etc.*; Tolosa *et al.*, 1999). Moreover, re-engineering the binding site of these proteins as a designed scaffold may significantly expand the number of small-molecule analytes for which sensors may be generated. In this framework, it is evident that proteins isolated from thermophilic organisms possess added intrinsic value in the design of new biosensing technologies that require enhanced stability.

Recently, we characterized a PBP that is involved in the amino-acid transport system of *Thermotoga maritima* (Luchansky *et al.*, 2010; Scirè *et al.*, 2010). Integrated biochemical and biophysical characterization of this protein (hereafter referred to as TmArgBP) has shown that it is an arginine-binding protein that is endowed with remarkable structural stability even under strongly denaturating conditions. Indeed, the native protein could not be denatured when

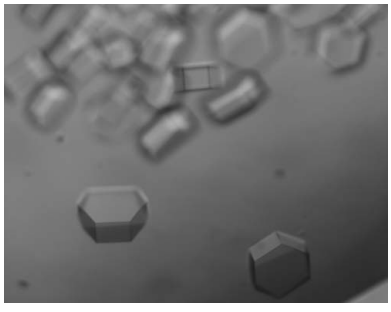

Table 1
Data-collection parameters and data-processing statistics.

Values in parentheses are for the highest resolution shell.

	HoloTmArgBP	ApoTmArgBP
Radiation source	Beamline X12, EMBL/DESY	In-house rotating anode
Wavelength (Å)	1.000	1.5418
Crystal-to-detector distance (mm)	260	55
Oscillation angle per frame (°)	0.10	0.50
Crystal symmetry and presumed space group	Hexagonal, $P622$	Orthorhombic, $P2_12_12_1$
Unit-cell parameters (Å)	a = 78.2, b = 78.2, c = 434.7	a = 51.8, b = 91.9, c = 117.9
Resolution (Å)	50.0–2.70 (2.80–2.70)	50.0–2.25 (2.33–2.25)
Mean multiplicity	3.2	4.7
Completeness (%)	94.0 (79.7)	89.7 (85.5)
Total reflections	68279	115134
Unique reflections	21612	24691
$R_{\rm merge}$†	0.124 (0.356)	0.126 (0.242)
Mean $I/\sigma(I)$	11.6 (2.7)	14.0 (5.2)

† $R_{\rm merge} = \sum_{hkl}\sum_i |I_i(hkl) - \langle I(hkl)\rangle| / \sum_{hkl}\sum_i I_i(hkl)$, where $I_i(hkl)$ is the intensity of the ith measurement of reflection hkl and $\langle I(hkl)\rangle$ is the mean value of the intensity of reflection hkl.

heated to 373 K. Moreover, it is quite stable ($T_{\rm m}$ of 351 K) even when treated with 6.0 *M* guanidinium hydrochloride. On this basis, it has been suggested that this ultrastable protein has the potential to be exploited for the generation of durable and highly specific sensors for arginine. The structural characterization of TmArgBP at the atomic level will therefore be extremely useful for potential biotechnological applications of this protein and for elucidation of the determinants of its exceptional stability. Moreover, structural studies will also provide useful insights into the interfaces involved in the mixture of oligomeric states (homodimers and homotrimers) detected for TmArgBP. Here, we report the crystallization and preliminary crystallographic investigations of TmArgBP.

2. Experimental methods

2.1. Cloning, expression and purification

In previous characterizations of TmArgBP, a construct presenting an extension of 22 residues at the C-terminus, including a 6×His-tag motif, was used. To increase the crystallizability of the protein, a new construct was prepared by the insertion of a stop codon that removes this C-terminal extension. This construct, which was also deprived of the signal sequence for perisplasmic export of the protein, corresponds to the region 20–246 (227 residues) of the protein sequence (UniProt code Q9WZ62). This sequence region was cloned into the *Nde*I–*Bam*HI site of a pET21a vector. The resulting positive plasmid was used to transform Rosetta(DE3)pLysS competent cells. Expression of the protein was carried out using the transformed cells, which were grown overnight at 310 K in LB containing 50 µg ml^{-1} kanamycin and 30 µg ml^{-1} chloramphenicol. When an OD_{600} of 0.6 was reached, the cells were induced for 3 h with 0.5 m*M* IPTG.

The absence of the 6×His affinity tag from the present TmArgBP construct required some modifications of the protein-purification protocol. The cells were resuspended in 20 m*M* Tris–HCl buffer pH 8.0 containing a protease-inhibitor cocktail (Roche Diagnostic) and sonicated. The cell debris was removed by centrifugation at 18 000 rev min^{-1} for 40 min. The protein supernatant was initially purified by thermoprecipitation (343 K water bath for 30 min). The heat-denatured proteins were removed by centrifugation. The soluble protein extract was loaded onto a 5 ml Resource Q column (Pharmacia) equilibrated with Tris buffer pH 8.0. After washing with ten volumes of buffer, a linear gradient of NaCl (0–500 m*M*) was applied to elute the protein. The fractions containing TmArgBP were pooled and dialyzed against a buffer consisting of 20 m*M* Tris–HCl pH 8.0, 150 m*M* NaCl at 277 K. After dialysis, the protein was concentrated for further purification by size-exclusion chromatography on Superdex 200 (GE Healthcare; 50 m*M* Tris–HCl, 150 m*M* NaCl pH 8.0). The homogeneity of the protein was evaluated by SDS–PAGE analysis. The molecular mass of the purified protein (25 270 Da) was checked by mass spectrometry and no proteolysis of the protein was detected.

2.2. Crystallization experiments

Crystallization trials were performed at 293 K using the hanging-drop vapour-diffusion method. A preliminary screening for crystallization conditions was carried out using commercially available sparse-matrix kits (Crystal Screen, Crystal Screen 2 and Index from Hampton Research; Jancarik & Kim, 1991). Optimization of the crystallization conditions was performed by fine-tuning the protein and precipitant concentrations and by the use of crystallization additives (Additive Screen from Hampton Research; McPherson *et al.*, 2011).

2.3. Data collection and processing

Preliminary diffraction data for both the apo and holo forms of TmArgBP were collected in-house at 100 K using a Rigaku MicroMax-007 HF generator producing Cu $K\alpha$ radiation and equipped with a Saturn944 CCD detector. This equipment was also used for

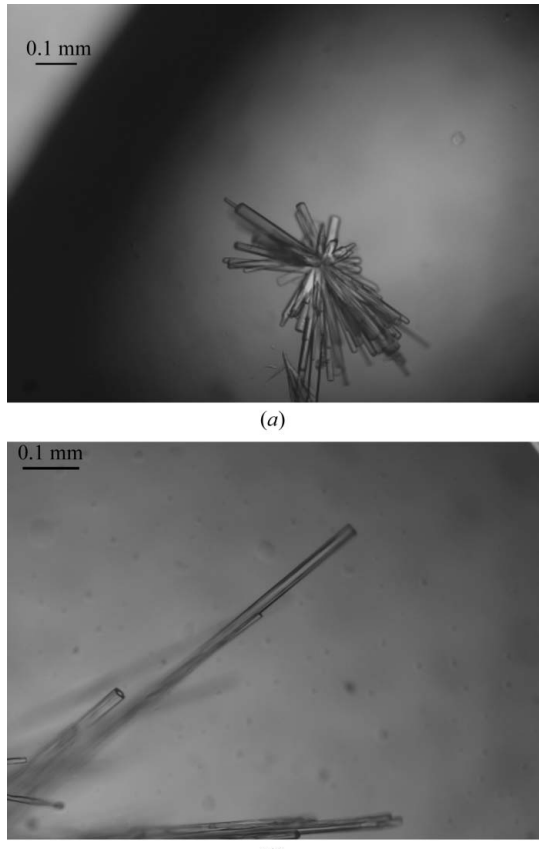

Figure 1
(*a*) Crystals of HoloTmArgBP grown in 17%(*w*/*v*) PEG 10 000, 0.1 *M* bis-tris pH 5.5, 0.1 *M* ammonium acetate. The crystals shown in (*b*) were grown under the same conditions with the addition of LDAO detergent [0.5%(*v*/*v*)].

the collection of the diffraction data from the apo form. Data were collected at 100 K from crystals cryoprotected by adding a solution of 14%(*v*/*v*) ethylene glycol to the precipitating solution. Diffraction data for the holo form of TmArgBP were collected on the X12 synchrotron beamline at the DORIS storage ring, DESY (Hamburg, Germany) using a MAR225 CCD detector at 100 K from crystals cryoprotected by adding 14%(*v*/*v*) ethylene glycol to the precipitating solution. The diffraction data were collected using a small rotation angle of 0.1° and a crystal-to-detector distance of 260 mm owing to the long *c* axis.

All data sets were scaled and merged using the *HKL*-2000 program package (Otwinowski & Minor, 1997). Statistics of data collection are reported in Table 1.

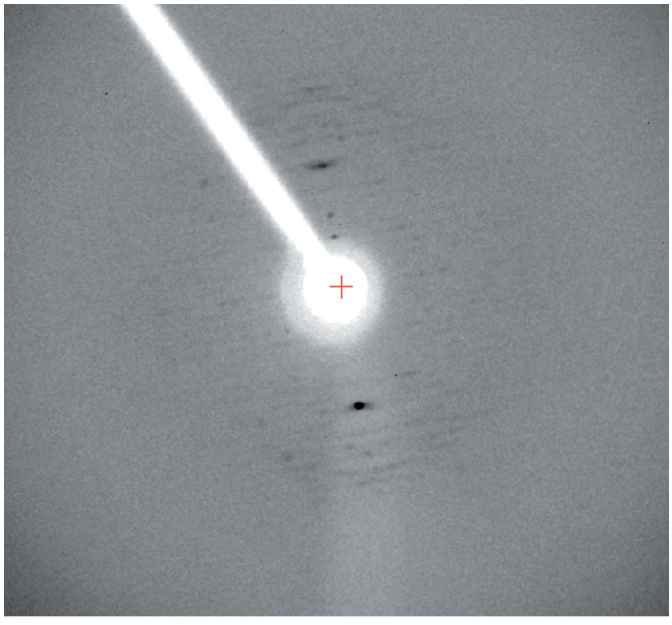

(*a*)

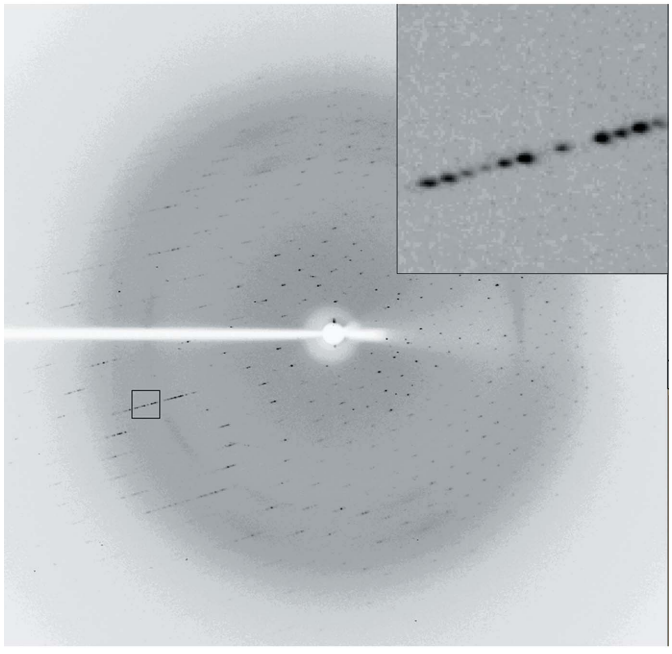

(*b*)

Figure 2
Diffraction patterns of HoloTmArgBP crystals obtained in the absence (*a*) or in the presence (*b*) of the additive LDAO.

3. Results and discussion

Previous characterizations of TmArgBP have clearly indicated that the protein purifies as a complex with arginine. Analysis of the thermal stability of the TmArgBP sample obtained using the purification procedure adopted here demonstrates that it also corresponds to the arginine-bound complex (HoloTmArgBP). The protein does not unfold in aqueous solutions when heated to 373 K. Thermal denaturation was observed at 351 K when 6.0 *M* guanidinium hydrochloride was added to the solution, in line with previous analyses carried out on the arginine-bound complex.

An initial screening of commercially available solutions provided promising crystallization conditions for HoloTmArgBP in the presence of PEG 10 000 as a precipitant. The size and morphology of the HoloTmArgBP crystals were improved by fine-tuning the concentrations of the protein and the precipitating agent. Crystals that were suitable for diffraction experiments were obtained using vapour-diffusion techniques and a protein concentration of 20–25 mg ml^{-1}. The composition of the reservoir solution was 17%(*w*/*v*) PEG 10 000, 0.1 *M* ammonium acetate, 0.1 *M* bis-tris buffer pH 5.5. Despite their good morphology (Fig. 1*a*), these crystals were highly disordered, as shown by their fibre-like diffraction pattern (Fig. 2*a*). In order to improve the quality of these crystals, a number of additives were added to the crystallization drops. Long rod-shaped crystals (0.05 × 0.1 × 0.6 mm) were obtained using 0.5%(*w*/*v*) *n*-dodecyl-*N*,*N*-dimethylamine-*N*-oxide (LDAO) as an additive (Fig. 1*b*). These crystals reached their optimal size in 1 d. Analysis of the diffraction pattern exhibited by these new crystals clearly indicated that the additive greatly improved the crystal quality (Fig. 2*b*). Indexing of the

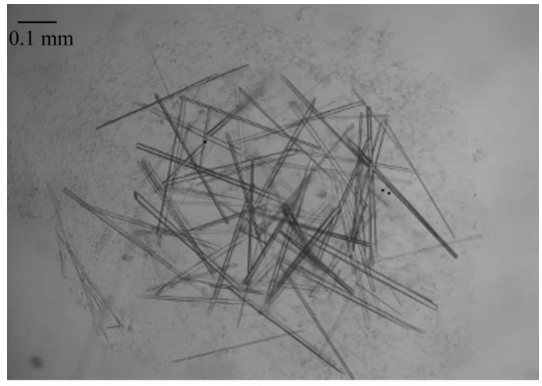

(*a*)

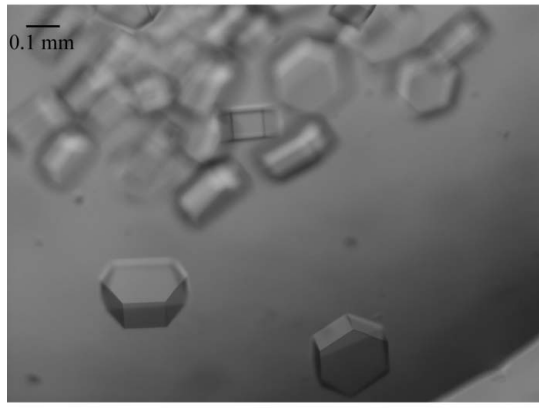

(*b*)

Figure 3
Crystals of ApoTmArgBP grown in the presence of (*a*) 20%(*w*/*v*) PEG 3350, 0.1 *M* HEPES pH 7.5, 0.15 *M* ammonium acetate and (*b*) 20%(*w*/*v*) PEG MME 2000, 0.1 *M* Tris–HCl pH 8.5, 0.2 *M* trimethylamine *N*-oxide dihydrate.

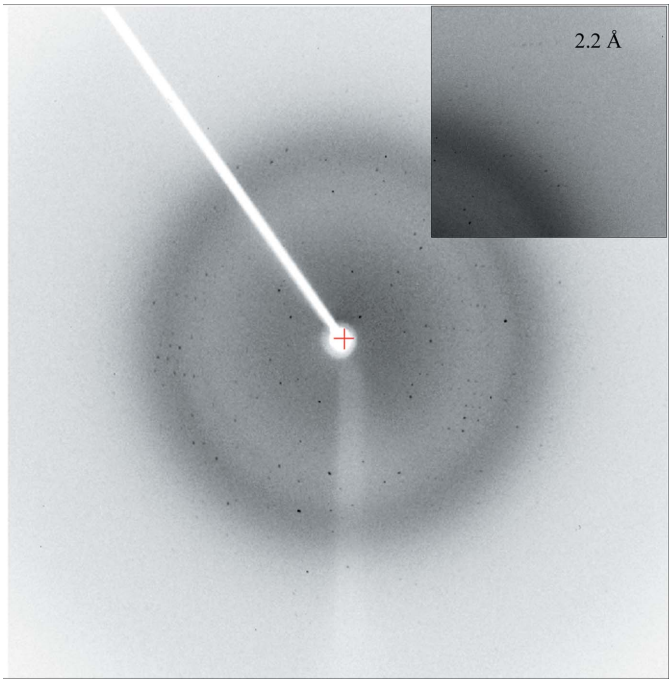

Figure 4
Diffraction pattern of ApoTmArgBP crystals grown in 20%(*w*/*v*) PEG 3350, 0.1 *M* HEPES pH 7.5, 0.15 *M* ammonium acetate.

diffraction pattern demonstrated that these crystals present a very long unit-cell axis (~435 Å; Fig. 2*b* and Table 1). To avoid overlaps of diffraction spots, a long crystal-to-detector distance (260 mm) was used for data collection. Moreover, although the long axis of the crystal was almost parallel to the spindle axis, we prudently used a small oscillation range (0.1°). The crystals presented a primitive hexagonal symmetry. Statistics of data processing and scaling are reported in Table 1, assuming space group *P*622. Matthews coefficient calculations (Matthews, 1968) suggest the presence of either three (V_M = 2.5 Å^3 Da^{-1}, 51% solvent content) or four (V_M = 1.9 Å^3 Da^{-1}, 35% solvent content) molecules per asymmetric unit.

The apo form of the protein (ApoTmArgBP) was prepared using the procedure reported by Luchansky *et al.* (2010). Briefly, the protein was incubated with 6.0 *M* guanidinium hydrochloride under dialysis for 3 d. The denaturant was removed by dialysis (Luchansky *et al.*, 2010) against a solution consisting of 20 m*M* Tris–HCl, 150 m*M* NaCl pH 8.0. The melting temperature (336 K) of this protein sample in 6.0 *M* guanidinium hydrochloride was virtually identical to that exhibited by the apo form in previous studies (Luchansky *et al.*, 2010). Crystallization screenings performed using commercial kits led to the identification of several promising crystallization conditions. Crystals suitable for X-ray diffraction testing were obtained using either 20%(*w*/*v*) PEG 3350, 0.1 *M* HEPES pH 7.5, 0.15 *M* ammonium acetate or 20%(*w*/*v*) PEG MME 2000, 0.1 *M* Tris–HCl pH 8.5, 0.2 *M* trimethylamine *N*-oxide dihydrate (Figs. 3*a* and 3*b*) as precipitating solutions. In both cases the protein concentration was in the range 15–20 mg ml^{-1}. The crystals obtained from the solution containing PEG MME 2000 displayed a poor diffraction pattern (lower than 6 Å resolution) despite their good morphology (Fig. 3*b*). In contrast, the crystals obtained using PEG 3350 as precipitant proved to be suitable for crystallographic data collection (Fig. 4). These crystals reached their optimal size within one week. The crystals were orthorhombic, with unit-cell parameters *a* = 51.8, *b* = 91.9, *c* = 117.9 Å, and diffracted to 2.25 Å resolution (Table 1). Matthews coefficient calculations suggested the presence of two molecules (V_M = 2.8Å^3 Da^{-1}, 56% solvent content) per asymmetric unit (Matthews, 1968).

Attempts to solve the structures of both the apo and holo forms of the protein are in progress. In particular, models of ArgBP isolated from *Salmonella typhimurium* (Stamp *et al.*, 2011) and *Geobacillus stearothermophilus* (Vahedi-Faridi *et al.*, 2008), which share ~37% sequence identity with TmArgBP, are being used in the trials. As molecular-replacement trials may be complicated by the large unit cell of the holo form and by the intrinsic flexibility of amino-acid-binding proteins in their ligand-free state, selenomethionine derivatives of TmArgBP are being prepared.

This work was funded by the MIUR (FIRB Contract No. RBRN07BMCT). We acknowledge the staff of beamline X12 at EMBL/DESY (Hamburg, Germany) for providing the synchrotron-radiation facilities and for valuable assistance during data collection. We also thank Ms Flavia Squeglia for her help during sample preparation.

References

Davidson, A. L., Dassa, E., Orelle, C. & Chen, J. (2008). *Microbiol. Mol. Biol. Rev.* **72**, 317–364.
Ethayathulla, A. S., Bessho, Y., Shinkai, A., Padmanabhan, B., Singh, T. P., Kaur, P. & Yokoyama, S. (2008). *Acta Cryst.* F**64**, 498–500.
Higgins, C. F. (1992). *Annu. Rev. Cell Biol.* **8**, 67–113.
Jancarik, J. & Kim, S.-H. (1991). *J. Appl. Cryst.* **24**, 409–411.
Lorimier, R. M. de, Smith, J. J., Dwyer, M. A., Looger, L. L., Sali, K. M., Paavola, C. D., Rizk, S. S., Sadigov, S., Conrad, D. W., Loew, L. & Hellinga, H. W. (2002). *Protein Sci.* **11**, 2655–2675.
Luchansky, M. S., Der, B. S., D'Auria, S., Pocsfalvi, G., Iozzino, L., Marasco, D. & Dattelbaum, J. D. (2010). *Mol. Biosyst.* **6**, 142–151.
Marvin, J. S., Corcoran, E. E., Hattangadi, N. A., Zhang, J. V., Gere, S. A. & Hellinga, H. W. (1997). *Proc. Natl Acad. Sci. USA*, **94**, 4366–4371.
Matthews, B. W. (1968). *J. Mol. Biol.* **33**, 491–497.
McPherson, A., Nguyen, C., Cudney, R. & Larson, S. B. (2011). *Cryst. Growth Des.* **11**, 1469–1474.
Nanavati, D. M., Nguyen, T. N. & Noll, K. M. (2005). *J. Bacteriol.* **187**, 2002–2009.
Oldham, M. L., Davidson, A. L. & Chen, J. (2008). *Curr. Opin. Struct. Biol.* **18**, 726–733.
Otwinowski, Z. & Minor, W. (1997). *Methods Enzymol.* **276**, 307–326.
Scirè, A., Marabotti, A., Staiano, M., Iozzino, L., Luchansky, M. S., Der, B. S., Dattelbaum, J. D., Tanfani, F. & D'Auria, S. (2010). *Mol. Biosyst.* **6**, 687–698.
Stamp, A. L., Owen, P., El Omari, K., Lockyer, M., Lamb, H. K., Charles, I. G., Hawkins, A. R. & Stammers, D. K. (2011). *Proteins*, **79**, 2352–2357.
Tolosa, L., Gryczynski, I., Eichhorn, L. R., Dattelbaum, J. D., Castellano, F. N., Rao, G. & Lakowicz, J. R. (1999). *Anal. Biochem.* **267**, 114–120.
Vahedi-Faridi, A., Eckey, V., Scheffel, F., Alings, C., Landmesser, H., Schneider, E. & Saenger, W. (2008). *J. Mol. Biol.* **375**, 448–459.